Bulgarian Chemical Communications, Volume 56, Issue 3 (pp. 321-327) 2024 DOI: 10.34049/bcc.56.3.BB-M

Optimization and determination of the factors influencing the delamination in graphene/MoS_2/PET nanocomposite under mechanical loading

B. Boyadjiev [1]*, T. Petrova [1], R. Vladova [1], E. Kirilova [1], A. Apostolov [1], A. Moravski[2]

[1] *Institute of Chemical Engineering, Bulgarian Academy of Sciences,Acad. G. Bonchev Str., Bl.103, 1113 Sofia, Bulgaria*

[2] *Faculty of Mathematics and Informatics, Sofia University "St. Kliment Ohridski",5 James Bourchier Blvd., 1164 Sofia, Bulgaria*

Receoved June 3, 2024; Accepted: August 17, 2024

The current theoretical study is devoted to the identification of the factors influencing the interface shear stress and respectively, the possibility of delamination appearing in three-layer nanocomposite structure graphene/MoS_2/PET under mechanical loading. A model criterion for delamination in the structure is proposed and the model interface shear stress is calculated at different geometry and external loads [1]. Then, a multi-parametric optimization procedure is performed which shows the exact geometrical and external factors influencing the interface shear stress value – layer's thickness, load and length of the considered nanocomposite structure. The obtained results could be used to predict the safe design and working conditions in similar nanocomposite devices or parts of them, as sensors, nano- and optical electronic devices, energy devices, etc.

Keywords*:* Multi-parameter optimization; graphene/MoS_2/PET nanocomposite; interface shear stress; delamination.

INTRODUCTION

In the last ten years, the combinations of two and more 2D nanomaterials with different substrates, and respectively, the investigation of their properties, are in the focus of scientists in the world [3, 4, 6-10]. In [3, 4] and [7, 10] graphene/MoS_2 or WS_2/MoS_2 were combined with polymers or Si/SiO_2 as parts of different electronic and sensor devices, etc. The obtained heterostructures and their properties, were studied mostly experimentally. The performance gain-oriented nano-structurization has opened a new pathway for tuning mechanical features of solid matter vital for application and maintained performance [8].

The 2D materials and their heterostructures offer excellent mechanical flexibility, optical transparency, and favorable transport properties for realizing electronic, sensing, and optical systems on arbitrary surfaces [4, 9]. The mechanical and physical properties of those heterostructures formed by stacking different two-dimensional materials show great potential for the next generation of electronic and optoelectronic materials. But, the interfacial mechanical behavior of those heterostructures with different substrates is still a critical problem in various fields [3, 10]. Understanding the mechanical properties and critical limits for safety work (without failure) in the structure is extremely significant in the engineering [3].

The aim of this work is to find the optimal values of geometry (length and thicknesses of all three layers), as well as the maximal value of external load in graphene/MoS_2/PET nanocomposite under mechanical loading, without delamination in it. The analytical solutions for ISS and model criteria guaranteeing no delamination in the nanocomposite [1] are implemented in the multi-parameter optimization problem. Two optimization procedures (with genetic algorithms [2] and Mathematica) were defined and solved with objective function – the model criteria for ISS limit. As a result, different sets of optimal geometry configurations of the layers (length and thicknesses of all three layers) and optimal load in the considered nanocomposite structure, have been obtained.

Mathematical model

The mathematical model of the representative volume element (Fig. 1) of the three-layer statically loaded nanocomposite structure graphene/MoS_2/PET describing the axial shear stress $\sigma_1(x)$ is created using a two-dimensional stress-function method [1]. The model is described with the fourth-order ordinary differential equation (ODE) (1) with constant coefficients D_i:

$$2D_2\sigma_1'''' + (2-2D_4)\sigma_1'' + 2D_1\sigma_1 + D_5 = 0 \qquad (1)$$

* To whom all correspondence should be sent:
E-mail: *boyan.boyadjiev@iche.bas.bg*

This mathematical model is created by making the following model assumptions:

1. The axial stresses in the layers are assumed to be functions of axial coordinate x only.

2. In the MoS_2 interface layer the axial stress is negligible in respect to the same ones in the other two layers.

3. All stresses in the layers (axial, normal (peel) and shear stresses) are determined under the assumption of the plane-stress formulation.

The interface layer is simulated by the approach in [5].

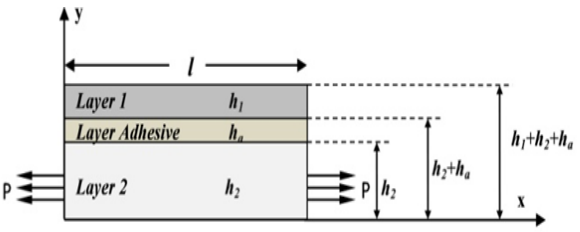

Fig. 1. Representative volume element of the three-layer nanocomposite structure. Layer 1 – graphene, Layer interface – MoS_2, Layer 2 - PET

Boundary and contact conditions for stresses $\sigma_{xx}^{(i)}, \sigma_{xy}^{(i)}, \sigma_{yy}^{(i)}$ of the layers $i = 1, \mathrm{a}, 2$ are:

For layer (1):

$$\sigma_{xx}^{(1)} = \begin{cases} 0 & \text{if } x = 0 \\ 0 & \text{if } x = l \end{cases};$$
$$\sigma_{xy}^{(1)} = \begin{cases} 0 & \text{if } x = 0 \\ 0 & \text{if } x = l \end{cases}; \tag{2}$$
$$y \in \left[h_2 + h_a, h_1 + h_2 + h_a\right].$$

$$\sigma_{yy}^{(1)} = \begin{cases} 0 & \text{if } y = h_1 + h_2 + h_a \\ \sigma_{yy}^{(\mathrm{a})} & \text{if } y = h_2 + h_a \end{cases};$$
$$\sigma_{xy}^{(1)} = \begin{cases} 0 & \text{if } x = h_1 + h_2 + h_a \\ \sigma_{xy}^{(\mathrm{a})} & \text{if } x = h_2 + h_a \end{cases}; \quad x \in [0, l]. \tag{3}$$

For layer (a):

$$\sigma_{xx}^{(a)} = \begin{cases} 0 & \text{if } x = 0 \\ 0 & \text{if } x = l \end{cases};$$
$$\sigma_{xy}^{(a)} = \begin{cases} 0 & \text{if } x = 0 \\ 0 & \text{if } x = l \end{cases}; \tag{4}$$
$$y \in \left[h_2, h_2 + h_a\right].$$

$$\sigma_{yy}^{(\mathrm{a})} = \begin{cases} \sigma_{yy}^{(1)}\left(x, h_2 + h_a\right) & \text{if } y = h_2 + h_a \\ \sigma_{yy}^{(2)}\left(x, h_2\right) & \text{if } y = h_2 \end{cases};$$
$$\sigma_{xy}^{(\mathrm{a})} = \begin{cases} \sigma_{xy}^{(1)}\left(x, h_2 + h_a\right) & \text{if } y = h_2 + h_a \\ \sigma_{xy}^{(2)}\left(x, h_2\right) & \text{if } y = h_2 \end{cases}; \tag{5}$$
$$x \in [0, l].$$

For layer (2):

$$\sigma_{xx}^{(2)} = \begin{cases} \sigma_0 & \text{if } x = 0 \\ \sigma_0 & \text{if } x = l \end{cases};$$
$$\sigma_{xy}^{(2)} = \begin{cases} 0 & \text{if } x = 0 \\ 0 & \text{if } x = l \end{cases}; \tag{6}$$
$$y \in \left[0, h_2\right].$$

$$\sigma_{yy}^{(2)} = \begin{cases} \sigma_{yy}^{(\mathrm{a})}\left(x, h_2\right) & \text{if } y = h_2 \\ 0 & \text{if } y = 0 \end{cases};$$
$$\sigma_{xy}^{(2)} = \begin{cases} \sigma_{xy}^{(\mathrm{a})}\left(x, h_2\right) & \text{if } y = h_2 \\ 0 & \text{if } y = 0 \end{cases}; \tag{7}$$
$$x \in [0, l].$$

The analytical solution of the ODE equation (1) for the axial stress $\sigma_1(x)$ involves the discriminant of the respective characteristic equation. That discriminant can be either positive or negative, so the roots can be real or complex numbers, respectively. The sign of the discriminant depends on the thicknesses and material properties of the structure layers described by the coefficients D_i.

The possible general solutions of (1) for the axial stress $\sigma_1(x)$ are:

$$\sigma_1 = C_1\,\mathrm{e}^{\lambda_1 x} + C_2\,\mathrm{e}^{\lambda_2 x} + C_3\,\mathrm{e}^{\lambda_3 x} + C_4\,\mathrm{e}^{\lambda_4 x} - A. \tag{8}$$

$$\sigma_1 = \mathrm{e}^{-ax}\left[M_1 \cos(\beta x) + M_2 \sin(\beta x)\right] + \\ + \mathrm{e}^{ax}\left[M_3 \cos(\beta x) + M_4 \sin(\beta x)\right] - A. \tag{9}$$

where (8) is the solution for the case with 4 real roots λ_i and (9) is the solution for the case with 4 complex roots $\pm(\alpha \pm \mathrm{i}\beta)$.

In (8) and (9) C_i and M_i are the integration constants in the model solution, determined from the boundary conditions (2)–(7). The constant A is the solution for non-homogeneous ODE and depends on the external static load $\sigma_0 = P/h_2$ and Young's modulus and thicknesses of the first and third layer in the structure as $A = D_5/2D_1$ or:

$$A = \frac{\sigma_0 E^{(1)}}{\rho E^{(1)} + E^{(2)}}. \qquad (10)$$

After finding solution for axial stress σ_1, all other stresses in the layers of the considered graphene/MoS_2/PET structure can be obtained using this two-dimensional model relations:

$$\sigma_{xx}^{(1)} = \sigma_1(x) = \sigma_1, \quad \sigma_{yy}^{(1)} = \frac{1}{2}(y - y_t)^2 \sigma_1'',$$

$$\sigma_{xy}^{(1)} = (y_t - y)\sigma_1', \quad \sigma_{xx}^{(a)} \equiv 0, \quad \sigma_{xy}^{(a)} = h_1 \sigma'_{,1}$$

$$\sigma_{yy}^{(a)} = \left[\frac{h_1^2}{2} + h_1(c - y)\right]\sigma_1', \quad \sigma_{xx}^{(2)} = \sigma_0 - \rho\sigma_1,$$

$$\sigma_{yy}^{(2)} = \frac{-\rho}{2}\left[y^2 - y(y_t + h_a)\right]\sigma_1'', \quad \sigma_{xy}^{(2)} = \rho y \sigma_1',$$

where $\rho = h_1 / h_2$.

(11)

The model criterion without delamination in the considered interface layer of the nanostructure is:

$$\mathrm{ISS} = \sigma_{xy}^{(\mathrm{a})}(x) = h_1 \sigma_1' \le \sigma_{\mathrm{USS}}^{(\mathrm{a})}. \qquad (12)$$

where USS is the ultimate shear stress of the interface layer and ISS is the interface shear stress.

This criterion will be used for multi-parameter optimization to determine the model parameters.

Multi-parameter optimization problem

The parameters in the model criterion without delamination in graphene/MoS_2/PET are: length l, layers' thicknesses h_1, h_a, h_2 and external load σ_0. They are included in the coefficients D_i in equation (1) and in the integration constants C_i or M_i, depending of the type of model solution obtained from equation (8) or (9).

We use genetic algorithms [2] to find all 5 parameters l, h_1, h_a, h_2, and σ_0 which fulfill the criterion (12) and assure that there is no delamination in the graphene/MoS_2/PET nanocomposite.

The possible optimal solutions from the genetic algorithms represent a set of different combinations of all parameters, which vary within predefined boundaries, according to physical and technical prescriptions. The equation (12) is the objective function of the multi-parameter optimization and the abovementioned 5 parameters are the decision variables in the genetic algorithms. Those parameters are set to vary within predefined technological boundaries.

The block-scheme of genetic algorithms is presented on Fig. 2. In general, genetic algorithms are metaheuristics inspired by the process of natural selection in which population of individuals (candidate solutions) evolves toward better solution.

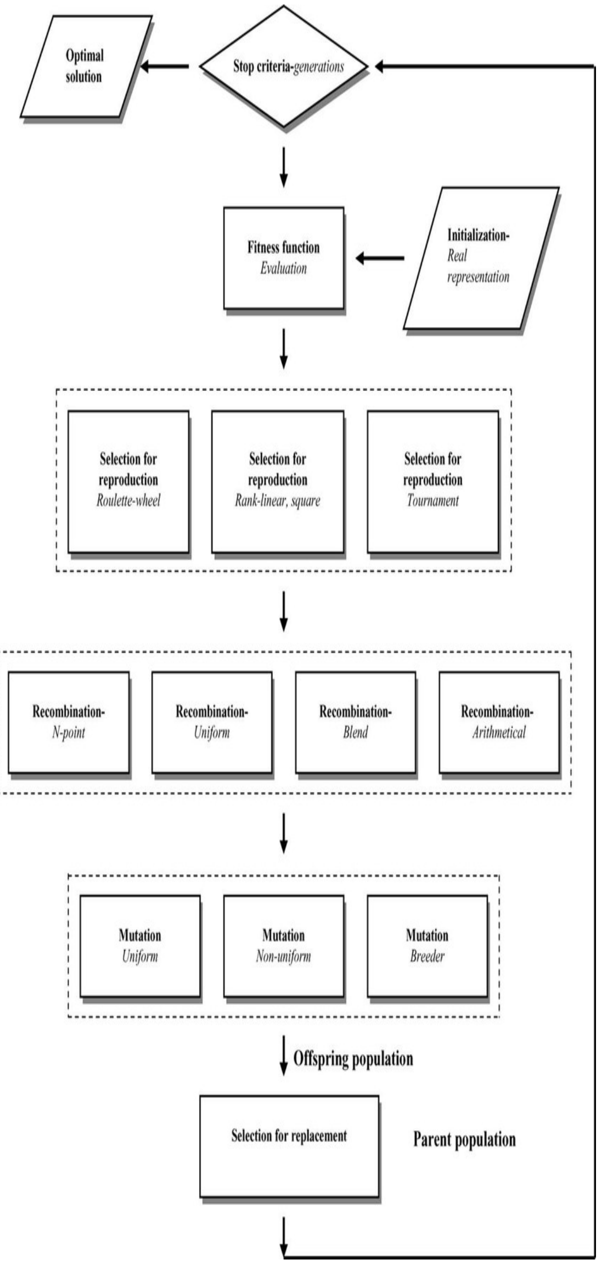

Fig. 2 Block-scheme of genetic algorithms [2]

Selection is the first stage of genetic algorithms, in which individuals are chosen from a population for later breeding. Selection mechanisms are also used to choose individuals for the next generation. There are several different methods of selection:

a. Roulette wheel selection. In the roulette wheel selection, the probability of choosing an individual for breeding of the next generation is proportional to its fitness, the better the fitness, the higher is the chance for that individual to be chosen. Choosing individuals can be depicted as spinning a roulette that has as many pockets as there are individuals in the current generation, with sizes depending on their probability. Probability p_i of choosing individual *i* is:

$$p_i = f_i \Big/ \sum_{j=1}^{n} f_i . \qquad (13)$$

where f_i is the fitness of and is the size of current generation. In this method one individual can be drawn several times. The principle of roulette wheel selection is shown on Fig. 3.

b. Tournament selection. Tournament selection is another genetic algorithms method of selecting a solution from a population of individuals. Tournament selection involves running several "tournaments" among a few individuals randomly choosed from the population. The winner of each tournament is the one with the best fitness, which is then selected for crossover. The probability of an individual to participate in the tornament depends on tournament size. If the tournament size is larger, weak individuals have a smaller chance to be selected, because, if a weak individual is selected to be in a tournament, there is a higher probability that a stronger individual is also in that tournament. The principle of tournament selection is shown on Fig. 4.

c. Selection for replacement. Often, to get better results, selection of replacement strategies with partial reproduction is used. One of them is elitism, in which a small portion of the best individuals from the last generation is carried over (without any changes) to the next one. Then the generation is complemented with new individuals and the whole process is repeated again. The principle of the selection for replacement is shown on Fig. 5.

RESULTS AND DISCUSSION

The mechanical properties of the heterostructure investigated in this work are presented in Table 1 and are given in [3].

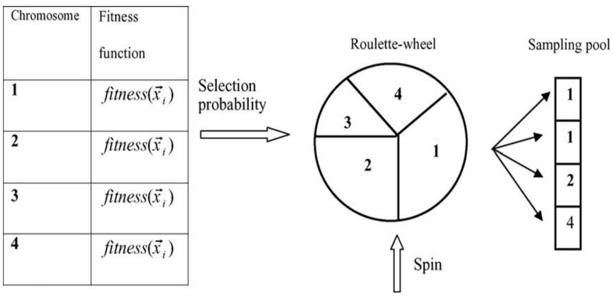

Fig. 3. Principle of roulette-wheel selection [2]

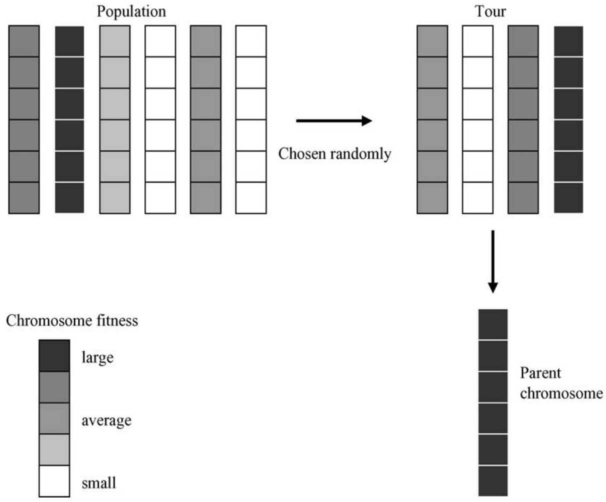

Fig. 4. Principle of tournament selection [2]

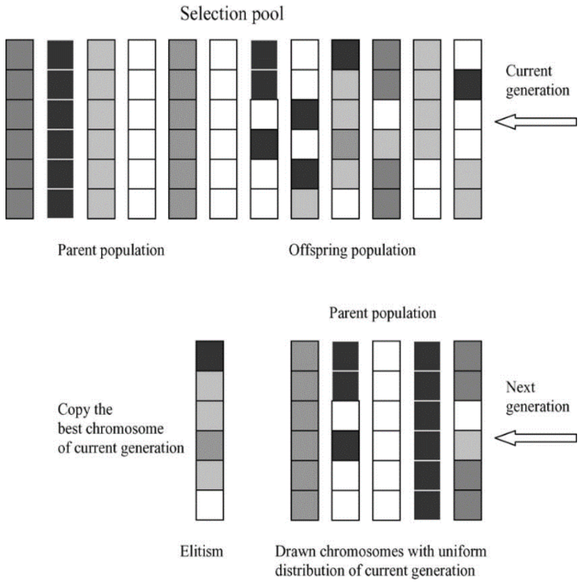

Fig. 5. Principle of the selection for replacement [2]

In Table 2 the obtained results from the performed GA multi-parameter optimization can be seen, for the case of complex roots solution for derivative of σ_1 in the objective function in eq. (12). For the case of real roots for ISS the alternative Mathematica optimization procedure was developed and solved with the same optimization criterion eq. (12). The results from Mathematica are presented in Table 3.

Table 1. Input data

Material	Young modulus, GPa	Poisson ratio
Graphene	1000	0.13
MoS_2	270	0.25
PET	2.3	0.43

Table 2. Obtained results from GA (complex roots).

Solution No.	1	2	3	4	5	6	8	9	10
Optimal load σ_0	2.84E+09	3.60E+09	3.74E+09	5.61E+09	1.53E+09	5.78E+09	2.77e+08	5.86e+09	4.70e+08
Optimal length l	1.76E-05	1.75E-05	1.73E-05	3.17E-05	1.87E-05	3.18E-05	7.49e-05	1.46e-05	4.48e-05
Optimal h_1	2.14E-09	3.05E-09	5.00E-09	3.82E-09	1.06E-09	4.49E-09	5.00E-09	4.81E-09	5.00E-09
Optimal h_a	1.00E-09	2.48E-09	1.00E-09	3.09E-09	3.61E-09	1.42E-09	6.83e-10	6.51e-10	6.65e-10
Optimal h_2	3.85E-04	4.15E-04	4.15E-04	8.70E-04	3.32E-04	8.81E-04	9.45e-04	4.64e-04	5.89e-04
GA population samples, generation, numbers	500 200 500	500 200 500	500 200 500	500 200 500	500 200 500	500 200 700	500 200 700	500 200 700	500 200 700
Methods used in GA*	TS, AC, NM	RWS, AC, NM	RWS, TPC, NM	TS, BC, NM	RS, BC, NM	TS, OPC, NM	TS, AC, NM	TS, AC, NM	TS, AC, NM

* Tournament selection, Arithmetical crossover, Non-uniform mutation (TS, AC, NM);
Roulette wheel selection, Arithmetical crossover, Non-uniform mutation (RWS, AC, NM);
Roulette wheel selection, Two-points crossover, Non-uniform mutation (RWS, TPC, NM);
Tournament selection, Blend crossover, Non-uniform mutation (TS, BC, NM);
Rank selection, Blend crossover, Non-uniform mutation (RS, BC, NM);
Tournament selection, One-point crossover, Non-uniform mutation (TS, AC, NM).

Table 3. Optimal values of parameters from Mathematica optimization procedure for graphene/MoS$_2$/PET (real roots)

Solution* No.	M2	M11	M12	M29	MLimit
Optimal load σ_0, MPa	1	1	0.182	1	0.95
Optimal l, m	1e-05	1e-05	1e-05	1.5e-05	1e-05
Optimal h_1, m	0.35e-09	0.675e-09	0.675e-09	0.35e-09	1e-09
Optimal h_a, m	1e-10	1e-10	1e-10	1e-10	1e-10
Optimal h_2, m	1e-06	1e-06	5.5e-06	1e-06	1e-06

* to differentiate the solutions in graphic results, these from Mathematica are noted with M

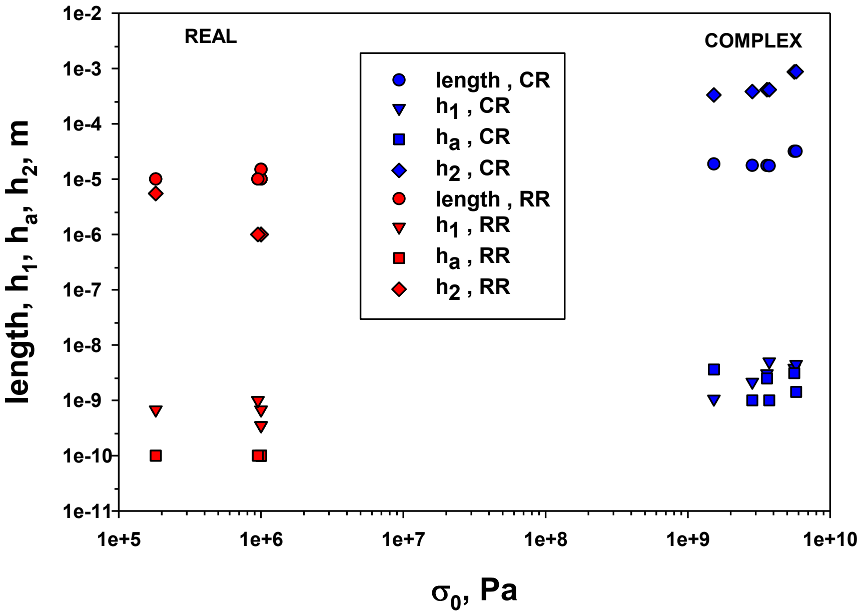

Fig. 6. Optimal solutions for 5 parameters from GA and Mathematica: complex roots CR (blue) and real roots RR (red)

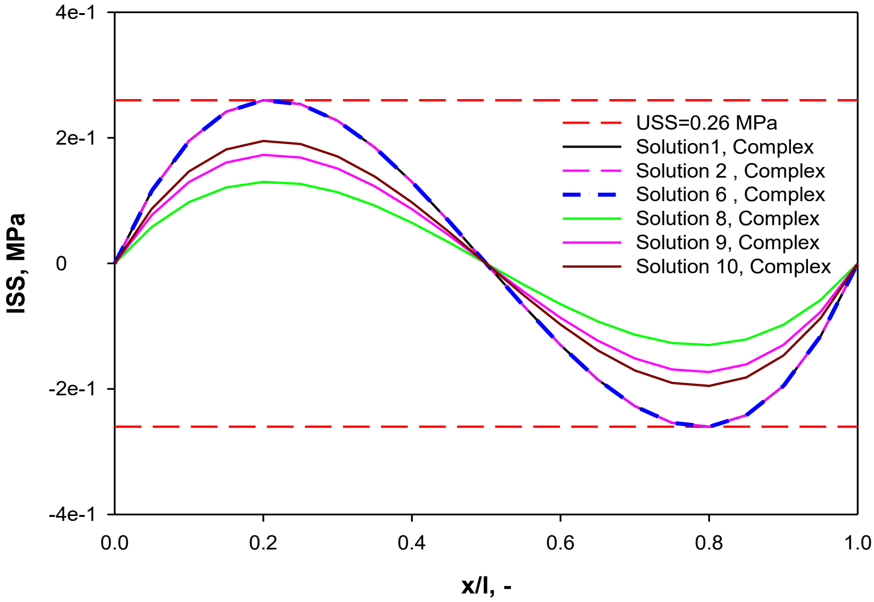

Fig. 7. Model Interface shear stress distribution calculated by the optimal values of parameters (complex roots)

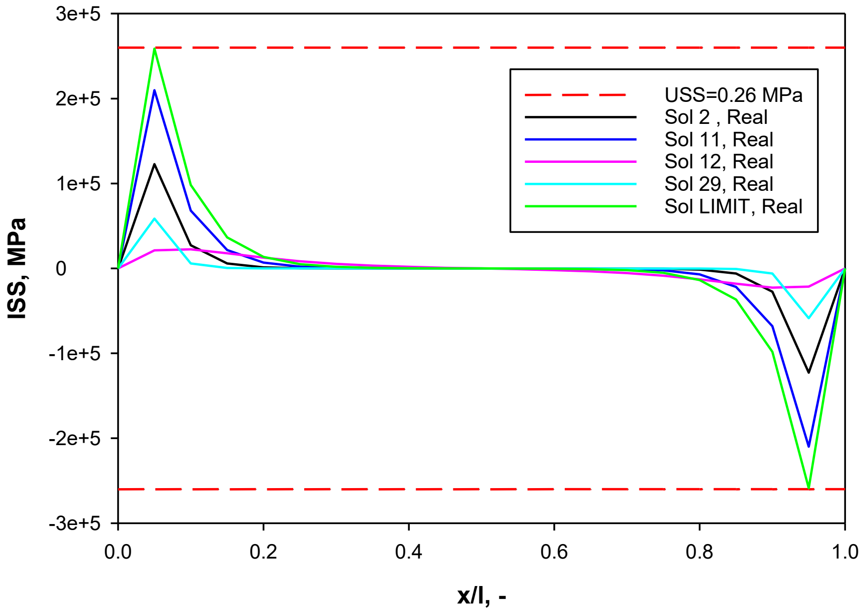

Fig. 8. Model interface shear stress distribution calculated at the optimal values of parameters (real roots)

In Figure 6, the sets of optimal values of the parameters (load, length, thicknesses of the three layers) are presented along with criterion equation (12) from both optimizations. It can be seen that along the ordinate each geometrical parameter changes within certain limits (intervals) for each of the two types of solutions (8) and (9) for ISS included in the objective function. The limits of the changes of the optimal thicknesses of PET h_2 and of the interface layer h_a, for the cases of real and complex roots, are particularly well differentiated. The intervals of variation of l are almost similar for both possible solutions (8) and (9). On the abscissa, each different set of geometry data corresponds to a particular mechanical load such that for each group of five parameters criterion (12) is met or the model-predicted ISS at these load and geometry values is equal to or below the critical USS value.

In order to verify the obtained results, the following Figures 7 and 8 present a part of the distributions of the ISS along the length of the nanocomposite obtained at the optimal values of the parameters. As can be seen, for each type of solution, the optimal values of the studied parameters actually meet the criterion of not having delamination in the nanocomposite structure. Graphically, on Figures 7 and 8, the ISS distribution for both cases does not exceed the straight horizontal line corresponding to the USS.

It turned out that the only data which can be compared with ours in the available literature, is the thickness of the interface layer – our common interval of obtained optimal values for h_a is (1e-10 ÷ 3.6e-09) for the investigated nanostructure. It is worth noting that the value obtained by Yu *et al*., 2014 [4] (0.8 nm) for graphene/MoS_2/Si is in the interval of the results obtained here, despite the different substrate used.

CONCLUSIONS

The multi-parameter optimization problem for three-layer nanostructure safety work (without delamination) is formulated and solved with genetic algorithms and Mathematica approach for axially loaded graphene/MoS_2/PET nanocomposite. The analytical model criterion based on the model ISS limit (no delamination), is included in the optimization procedures. The minimization of the later criteria as an objective function allows determining of the optimal values for 5 parameters: layers' thicknesses, length and mechanical loading for the considered nanocomposite.

The obtained optimal solutions represent a set of different combinations of all 5 parameters, which vary within predefined boundaries, according to physical and technical prescriptions.

The results show that at obtained optimal values of 5 parameters, the model ISSs confirmed and fulfilled the model criterion in graphene/MoS_2/PET. The obtained optimal interval of values for h_a coincides well with available literature data [4]. They could be used for predicting the optimal geometry design and load for any material combinations for three-layer nanocomposite structure, which satisfied the model assumptions [1].

Acknowledgement: *This study is performed by the financial support under the contract No. КП-06-Н57/3/15.11.2021 with Bulgarian National Science Fund for the project "Optimal safe loads and geometry for layered nanocomposites under thermo-mechanical loading ".*

Nomenclature

A - constant, solution of non-homogeneous ODE (1) of 4th order;

C_i, M_i - integration constants in the model solutions, determined from the respective boundary conditions;

E - Young modulus of layer material, Pa;

h_1, h_a, h_2 - thickness of the 1st, middle and 2nd layer in the nanocomposite, m ;

ISS - model interface shear stress, Pa;

l - length of the nanocomposite, m;

x, y P - applied tension force to the substrate, N.m;

- coordinate system, m;

USS - ultimate shear stress of middle layer in nanocomposite, Pa;

Greek symbols

λ_i - real roots of the characteristic equation corresponding to 4th order ODE;

$\pm(\alpha \pm i\beta)$ - complex roots of the characteristic equation corresponding to ODE of 4th order;

ν - Poisson number (ratio), - ;

σ_0 - external loading stress, applied to substrate, Pa;

$\sigma_1, \sigma^a_{x,y}$ - model axial and shear stress, Pa;

REFERENCES

1. T. S. Petrova, *Bulgarian Chemical Communications,* **55** (3), 349, (2023).
2. E. Shopova, N. Vaklieva-Bancheva, *Computers and Chemical Engineering*, **30**, 1293 (2006).
3. H. Du, Y., Kang, C., Xu, T., Xue, W., Qiu, H., Xie, *Optics and Lasers in Engineering*, **149**, 106825 (2022).
4. L. Yu, Yi-H. Lee, X. Ling, E. J. G. Santos, Y. C. Shin, Y. Lin, M. Dubey, E. Kaxiras, J. Kong, H. Wang, T. Palacios, *Nano Lett*., **14** (6), 3055 (2014).
5. L. Zhu, K. A. Narh, Composites, *Journal of Polymer Science Part B: Polymer Physics*, **42** (12), 2391 (2004).
6. A. Castellanos-Gomez, M. Poot, G.A. Steele, H.S.J. van der Zant, N. Agraït, G. Rubio-Bollinger, *Adv. Mater.*, **24**, 772 (2012).
7. B. Cho, J. Yoon, S. K. Lim, A. R. Kim, D.-H. Kim, S.-G. Park, J.-D. Kwon, Y.-J. Lee, K.-H. Lee, B. H. Lee, H. C. Ko, M. G. Hahm, *ACS Applied Materials and Interfaces*, **7** (30), 16775 (2015).
8. B. Graczykowski, M. Sledzinska, M. Placidi, D. S. Reig, M. Kasprzak, F. Alzina, C. M. S. Torres, *Nano Letters*, **17** (12), 7647 (2017).
9. S. Susarla, P. Manimunda, Y. M. Jaques, J. A. Hachtel, J. C. Idrobo, S. A. S. Amnulla, D. S. Galvão, C. S. Tiwary, P. M. Ajayan, *ACS Nano,* **12** (4), 4036 (2018).
10. H. Xing, X. Wang, C. Xu, H. Du, R. Li, Z. Zhao, W. Qiu, *Carbon*, **204**, 566 (2023).